PHYSICAL REVIEW E **74**, 060201(R) (2006)

Thermal rectifying effect in macroscopic size

B. Hu,[1,2] D. He,[1] L. Yang,[1,3,*] and Y. Zhang[1]

[1]*Department of Physics and The Beijing–Hong Kong–Singapore Joint Centre for Nonlinear and Complex Systems (Hong Kong), Hong Kong Baptist University, Kowloon Tong, Hong Kong, China*

[2]*Department of Physics, University of Houston, Houston, Texas 77204-5005, USA*

[3]*Institute of Modern Physics, Chinese Academy of Science, Lanzhou, China and Department of Physics, Lanzhou University, Lanzhou, China*

(Received 17 September 2005; published 8 December 2006)

We address the problem of the rectifying effect of heat conduction at macroscopic size. A design for a macroscopic thermal rectifier based on the macroscopic thermal conductivity of materials is introduced, and then realizations of the design are shown by numerical simulations and phenomenological estimations.

DOI: 10.1103/PhysRevE.74.060201 PACS number(s): 44.10.+i, 05.60.−k, 05.70.Ln

In recent years, the heat conduction in dynamical systems has attracted renewed attention. If the microscopic interactions between atoms are harmonic and then the phonons propagate ballistically, this will lead to thermal "superconduction." This means that the thermal conductivity κ diverges with increasing system size N, and Fourier's law is not obeyed. The thermal conductivity κ is defined as $\kappa = J/\Delta T$, where ΔT is the temperature difference at the two ends of the system, $J=jN$ is the total heat flux, and j is the heat flux. In 1914, Debye argued that nonlinearity in the interparticle forces is necessary for the finiteness of the thermal conductivity of insulating crystals. Later Peierls used the Boltzmann equation to show that anharmonicity is a necessary condition for Fourier's law to hold. Many nonlinear models have been studied to understand the effect of nonlinear microscopic interactions in heat conduction, and we are still far from a complete understanding [1–3]. Based on our understanding of nonlinear models, a potentially interesting application is to design a thermal rectifier for controlling the heat flow.

The study of electric currents has led to the invention of electric rectifiers, diodes, and transistors, and thus it is a crucial problem to design a thermal rectifier. A thermal rectifier has different total heat fluxes, as the rectifier is reversed between two heat baths. The absolute values of the two total heat fluxes are denoted as $J_{\pm}$, and $J_+ > J_-$. The ratio $r=J_+/J_-$ and the absolute value of J_+ describe the capability of the thermal rectifier, and $r \to 1$ or $J_+ \to 0$ represents that the thermal rectifier does not work. Very recently, several models of thermal rectifier have been studied [4–7]. For instance, Terraneo, Peyrard, and Casati [4] addressed a model where a strong Morse on-site potential lattice is sandwiched between two weak Morse on-site potential lattices. Li, Wang, and Casati [5] addressed a high-r model that consists of two Frenkel-Kontorova (FK) lattices coupled together by a harmonic spring with contact strength k. Hu and Yang [6] tried use of two FK lattices of different periodic on-site potentials to obtain a more effective thermal rectifier.

The models of a thermal rectifier consist of two or three layers; each layer is a different nonlinear lattice. For each layer, due to the nonlinear effect, the band of its effective phonon spectrum (the phonon band) will shift as its temperature changes. As a thermal rectifier is placed between two heat baths (temperature $T_{\pm}$, $T_+ > T_-$, $\Delta T = T_+ - T_-$), the phonon bands of the layers overlap and the heat can go through the thermal rectifier; as the thermal rectifier is reversed between the heat baths, the phonon bands of these layers become separated (the overlap vanishes) and the heat flow stops. So the mechanism of the thermal rectifier is that the overlap of the phonon bands changes to separation as the thermal rectifier is reversed.

These thermal rectifiers will work well as long as the system size N is small. However, as N increases, r will decrease dramatically [5,6,8–10]. This means that J_+ will not be notably bigger than J_-, when N is larger than a critical size N_c [9,10]. Although N_c will increase as k, the contact strength between two lattices, tends to zero, thermal rectifiers are hardly valid when N is a macroscopic size for any given k. On the other hand, for fixed N, $J_{\pm}$ depends on k with the relation $J_{\pm} \sim k^2$ as long as k is not big [5,9,10]. This means that $k \to 0$ leads to $J_+ \to 0$ faster. For increasing N, one needs to decrease k to keep $r \gg 1$. Thus, at macroscopic size, $r \gg 1$ and $J_+ \gg 0$ hardly hold at the same time. So, by the mechanism of the phonon band shift, it is more possible to design a mesoscopic or microscopic thermal rectifier, not a macroscopic one [9,10].

In this paper, we address the design of a thermal rectifier working at macroscopic size. The design is based on the macroscopic thermal conductivity of the material; see Fig. 1 for a schematic picture. The thermal rectifier consists of two segments: material A and material B. For material A, the thermal conductivity $\kappa_A(T)$ is an increasing function of T. For material B, the thermal conductivity $\kappa_B(T)$ is a decreasing function of T. When the thermal rectifier is placed in the situation BA or AB, the heat flux is denoted as J_+ or J_-. We focus on a simple case that $\kappa_A(T)$ crosses $\kappa_B(T)$ at $T=T_0$. The temperature of the right heat bath is $T_+ = T_0 + \Delta T/2$; the temperature of the left heat bath is $T_- = T_0 - \Delta T/2$. Then, for material B, κ_B in the situation BA is larger than for AB. For material A, κ_A in the situation BA is also larger than for AB. Thus we can expect that J_+ is larger than J_-. In this design, the macroscopic property of the material only is considered; the ratio r and absolute value of J_+ will be constants at the macroscopic size.

*Corresponding author.

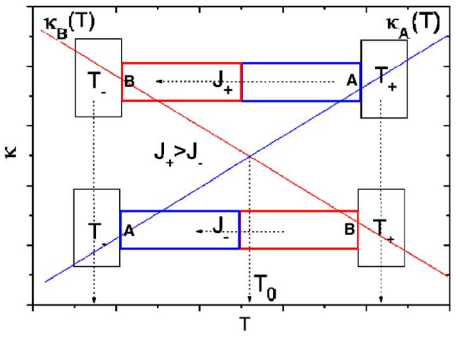

FIG. 1. (Color online) Schematic picture of the design of the thermal rectifier. $T_+ > T_-$ and $\Delta T = T_+ - T_-$.

For a realization of the design, the FK model and ϕ^4 model are considered. The Hamiltonian of the FK model is

$$H_{\mathrm{FK}} = \sum_i \left(\frac{p_i^2}{2m} + \frac{\lambda}{2}(q_{i+1} - q_i)^2 + \beta(1 - \cos q_i) \right); \qquad (1)$$

the Hamiltonian of the ϕ^4 model is

$$H_{\phi^4} = \sum_i \left(\frac{p_i^2}{2m} + \frac{\lambda}{2}(q_{i+1} - q_i)^2 + \frac{\alpha}{2} q_i^2 + \frac{\alpha}{4} q_i^4 \right), \qquad (2)$$

where $m=1$ is the mass of the particles, p_i the momentum of the ith particle, q_i its displacement from the equilibrium position, $\lambda=1$ the strength of the interparticle potential, and α and β the strength of the on-site potential. $\kappa(T)$ of the FK and ϕ^4 models are shown in Fig. 2 for $N=2048$. When the temperature is larger than 5, for the FK model, the thermal conductivity $\kappa_{\mathrm{FK}}(T)$ is an increasing function. For the ϕ^4 model, the thermal conductivity $\kappa_{\phi^4}(T)$ is a decreasing function. Here we take the FK model as the material A and the ϕ^4 model as the material B. The Hamiltonian of the thermal rectifier is

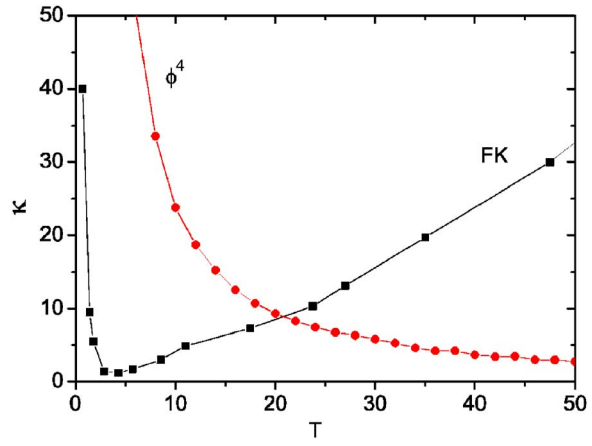

FIG. 2. (Color online) $\kappa(T)$ of FK and ϕ^4 models. For FK model, $\lambda=1$, $\beta=1.5$. For ϕ^4 model, $\lambda=1$, $\alpha=0.02$.

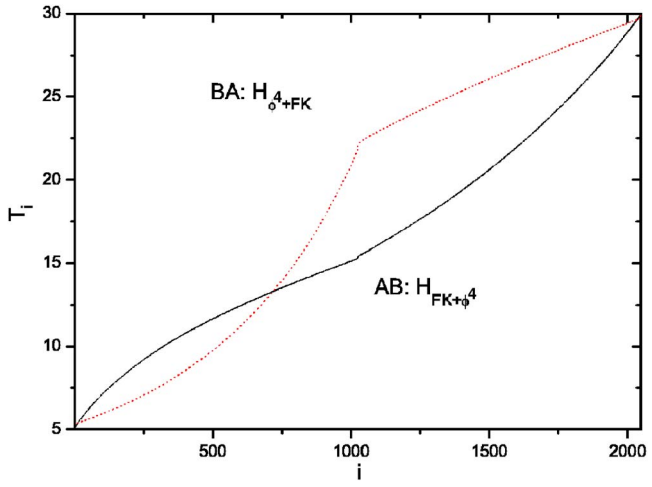

FIG. 3. (Color online) The temperature profiles. The left heat bath $T_+=30$, the right heat bath $T_-=5$. In $H_{\phi^4+\mathrm{FK}}$ and $H_{\mathrm{FK}+\phi^4}$, $\lambda=1$, $\alpha=0.02$, $\beta=1.5$.

$$H = H_{\phi^4+\mathrm{FK}} = \sum_{i=1}^{N/2} \left(\frac{p_i^2}{2} + \frac{\lambda}{2}(q_{i+1} - q_i)^2 + \frac{\alpha}{2} q_i^2 + \frac{\alpha}{4} q_i^4 \right) + \sum_{i=N/2+1}^{N} \left(\frac{p_i^2}{2} + \frac{\lambda}{2}(q_{i+1} - q_i)^2 + \beta(1 - \cos q_i) \right)$$

in the situation BA, and

$$H = H_{\mathrm{FK}+\phi^4} = \sum_{i=1}^{N/2} \left(\frac{p_i^2}{2} + \frac{\lambda}{2}(q_{i+1} - q_i)^2 + \beta(1 - \cos q_i) \right) + \sum_{i=N/2+1}^{N} \left(\frac{p_i^2}{2} + \frac{\lambda}{2}(q_{i+1} - q_i)^2 + \frac{\alpha}{2} q_i^2 + \frac{\alpha}{4} q_i^4 \right)$$

in AB.

Nonequilibrium molecular dynamics (NEMD) simulations are performed to investigate the model. Langevin thermostats are used in the NEMD simulations. More precisely, we simulate a chain of N_0+N+N_0 oscillators. The central N oscillators follow the Hamiltonian equations of motion while the outer $2N_0$ ones satisfy $q_i = -\partial H/\partial q_i - \gamma q_i + \xi_i$, where ξ_i is white Gaussian noise and $\langle \xi_i(t)\xi_k(t') \rangle = 2\gamma T_i \delta_{ik} \delta(t-t')$, where $T_i = T_+$ for $-N_0 \le i \le 0$ and $T_i = T_-$ for $N+1 \le i \le N+N_0$. In all simulations, $N_0=2$ and $\gamma=0.1$. The heat flux j takes the general expression for the heat flux [11]. Richardson's method is used for the integration [12]. The total integration time is typically $\cong 10^8 - 10^9$ units. The typical temperature profiles of the thermal rectifier are shown in Fig. 3. The dotted line shows the temperature profile of the thermal rectifier in situation BA ($H_{\phi^4+\mathrm{FK}}$); the solid line shows the temperature profile in situation AB ($H_{\mathrm{FK}+\phi^4}$). The results show that the temperature profiles are different and both are continuous.

We first study the thermal rectifier at a small size $N=128$ by NEMD simulations. Here, we take $\beta=1.5$, $\alpha=0.02$, and $T_\pm = T_0 \pm \Delta T$, where ΔT is an arbitrary parameter and changes from 1 to 20. In Fig. 4, $r(\Delta T)$ is shown for $T_0=6.0$, 10.0, 13.4, 16.0, and 20.0. It is clearly seen that r

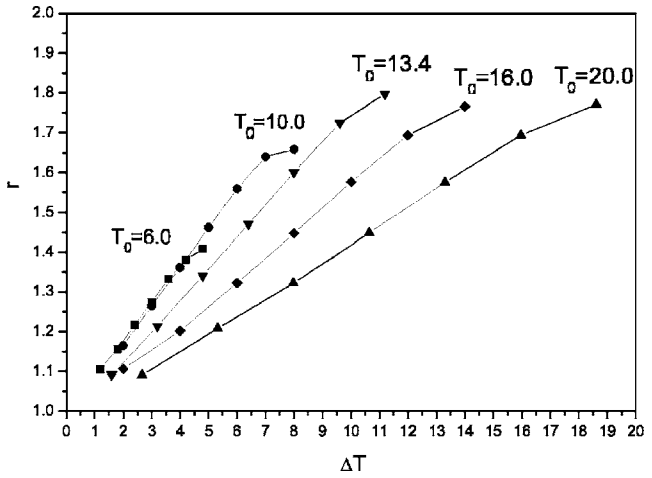

FIG. 4. Plot of $r(\Delta T)$ for different T_0. The system size $N=128$. In $H_{\phi^4+\mathrm{FK}}$ and $H_{\mathrm{FK}+\phi^4}$, $\lambda=1$, $\alpha=0.02$, $\beta=1.5$.

always increases with ΔT. Then, the finite-size effect is investigated; the relation between total heat fluxes $J_{\pm}$ and N is shown in Fig. 5 and $r(N)$in the inset. When $N<512$, $J_{\pm}$ and r increase with N. When $N>512$, $J_{\pm}$ and r approach constants; here $J_{+}\to 215$, $J_{-}\to 78$, $r\to 3$. The results are consistent with the expectation and the thermal rectifier does function properly at large size. We also investigate the possibility of other realizations of the design. It is known that the thermal conductivity $\kappa_{\mathrm{FPU}}(T)$ of Fermi-Pasta-Ulam (FPU) lattice is an increasing function [13] and the thermal conductivity $\kappa_{\mathrm{rotator}}(T)$ of the rotator model is a decreasing function [14]. We take the FPU model as the material A and the rotator model as the material B; similar conclusions are obtained.

Is it possible to construct a macroscopic thermal rectifier of two real materials, with phase diagrams of $\kappa(T)$ similar to Fig. 2? One can find similar phase diagrams in real solids, such as the quartz/diamond [15], sapphire/diamond [16], and quartz/GeN systems [17]. Here we take diamond as

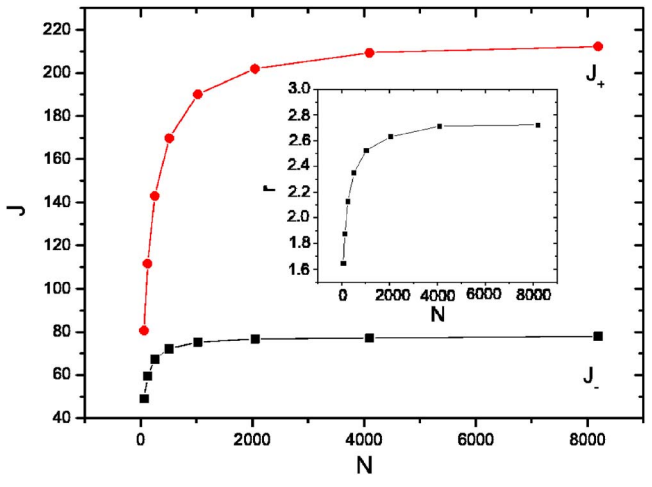

FIG. 5. (Color online) Plot of $J_{\pm}(N)$ and $r(N)$ in inset. The left heat bath $T_{+}=30$, the right heat bath $T_{-}=5$. In $H_{\phi^4+\mathrm{FK}}$ and $H_{\mathrm{FK}+\phi^4}$, $\lambda=1$, $\alpha=0.2$, $\beta=3.0$.

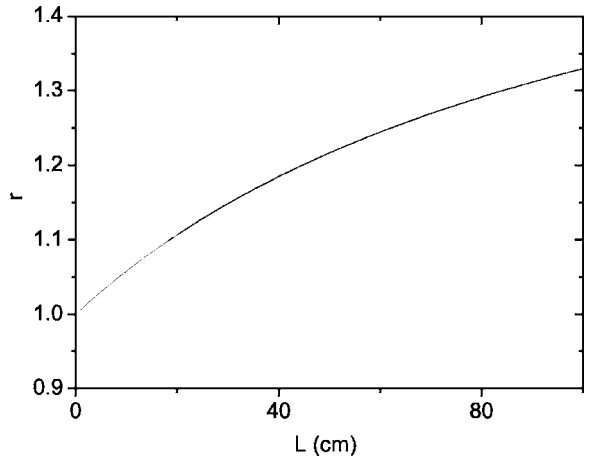

FIG. 6. Plot of r versus L (cm). $T_{+}=18$ K, $T_{-}=12$ K.

the material A and quartz as material B. $\kappa_{\mathrm{quartz}}(T)$ and $\kappa_{\mathrm{diamond}}(T)$ cross at $T\approx 15$ K. We choose the high temperature $T_{+}=18$ K, the low temperature $T_{-}=12$ K; for diamond $\kappa(12\ \mathrm{K})\approx 0.65\times 10^5\ \mathrm{W\ cm^{-1}\ K^{-1}}$, $\kappa(18\ \mathrm{K})\approx 1.1\times 10^5\ \mathrm{W\ cm^{-1}\ K^{-1}}$; for quartz $\kappa(12\ \mathrm{K})\approx 1.1\times 10^5\ \mathrm{W\ cm^{-1}\ K^{-1}}$, $\kappa(18\ \mathrm{K})\approx 0.65\times 10^5\ \mathrm{W\ cm^{-1}\ K^{-1}}$. Then we can use a general phenomenological formula [18] to estimate the thermal conductivity of the system, $\kappa=L/\{(L/2)[1/\kappa_{\mathrm{quartz}}(T)+1/\kappa_{\mathrm{diamond}}(T)]+R_b\}$; here L (cm) is the whole system size and R_b ($\mathrm{K\ cm^2\ W^{-1}}$) the boundary resistance, where we can estimate R_b from Refs. [18,19]. Thus, we obtain $r(L)$ shown in Fig. 6. The ratio r will increase with the system size, but the value is not very large. In addition, the boundary resistance R_b is very sensitive to the condition of the interface [19]; we speculate that it is not a very easy task to observe asymmetric heat conduction in the laboratory.

In summary, we present a design for the thermal rectifier based on the macroscopic property of the materials. Thus the thermal rectifier can function at the macroscopic size. The realization of the design is demonstrated by NEMD simulations in a model constructed using the FK and ϕ^4 models, and another realization can be constructed using the FPU and rotator models. For real materials, we give the example quartz/diamond, and then the rectifier effect is estimated by a general phenomenological formula. This study is not entirely academic; it opens possibilities of immediate technological importance. One example is to make a controlled temperature material in engineering applications [20]. One can more easily maintain an object at a desired temperature by using suitable material to enclose the object. If the object is a spacecraft or a satellite, material based on a thermal rectifier at macroscopic size will become more important. Although the possibility is still a completely open issue, our simulation results show a conceivable speculation.

We would like to thank members of the Centre for Nonlinear Studies for useful discussions. L.Y. acknowledges the support of the 100 Person Project of the Chinese Academy of Sciences. This work was supported in part by grants from the Hong Kong Research Grants Council (RGC) and the Hong Kong Baptist University Faculty Research Grant (FRG).

[1] F. Bonetto, J. L. Lebowitz, and L. Rey-Bellet, in *Mathematical Physics 2000* (Imperial College Press, London, 2000), p. 128.
[2] S. Lepri, R. Livi, and A. Politi, Phys. Rep. **377**, 1 (2003).
[3] T. Prosen and D. K. Campbell, Chaos **15**, 015117 (2005).
[4] M. Terraneo, M. Peyrard, and G. Casati, Phys. Rev. Lett. **88**, 094302 (2002).
[5] B. Li, L. Wang, and G. Casati, Phys. Rev. Lett. **93**, 184301 (2004).
[6] B. Hu and L. Yang, Chaos **15**, 015119 (2005).
[7] G. Casati, Chaos **15**, 015120 (2005); D. Segal and A. Nitzan, Phys. Rev. Lett. **94**, 034301 (2005); B. Xie, H. Li, and B. Hu, Europhys. Lett. **69**, 358 (2005).
[8] For the model of thermal rectifier in Ref. [4], the parameter k does not exist, so the discussions on k do not directly relate to the model. Here, we want to claim only that our NEMD simulation results show that r decreases from 1.93 to 1.05 as the size increases from $N=256$ to 2048.
[9] B. Hu, L. Yang, and Y. Zhang, Phys. Rev. Lett. **97**, 124302 (2006).
[10] B. Hu, D. He, L. Yang, and Y. ZhangPhys. Rev. E **74**, 060101 (2006).
[11] R. Kubo, M. Toda, and N. Hashitsume, *Statistical Physics II*, Springer Series in Solid State Sciences Vol. 31 (Springer, Berlin, 1991).
[12] J. Stoer and R. Bulirsch, *Introduction to Numerical Analysis* (Springer-Verlag, New York, 1980), Chap. 7, Sec. 2.14.
[13] K. Aoki and D. Kusnezov, Phys. Rev. Lett. **86**, 4029 (2001).
[14] O. V. Gendelman and A. V. Savin, Phys. Rev. Lett. **84**, 2381 (2000); L. Yang and B. Hu, *ibid.* **94**, 219404 (2005).
[15] R. Berman, F. E. Simon, and J. Wilks, Nature (London) **168**, 277 (1951).
[16] W. Liu and A. Balandin, J. Appl. Phys. **97**, 073710 (2005).
[17] R. Berman, *Thermal Conduction in Solids* (Clarendon Press, Oxford, 1979).
[18] E. Gmelin, M. Asen-Palmer, M. Reuther, and R. Villar, J. Phys. D **32**, R19 (1999).
[19] E. T. Swartz and R. O. Pohl, Rev. Mod. Phys. **61**, 605 (1989).
[20] P. Furmanski and J. M. Floryan, Int. J. Heat Mass Transfer **44**, 215 (2001); P. Furmanski and J. M. Floryan, ASME Trans. J. Heat Transfer **116**, 302 (1994).